Available online at www.sciencedirect.com
ScienceDirect
Journal of the European Ceramic Society 29 (2009) 1695–1701
www.elsevier.com/locate/jeurceramsoc

The thermal decomposition of $K_{0.5}Bi_{0.5}TiO_3$ ceramics

J. König *, M. Spreitzer, B. Jančar, D. Suvorov, Z. Samardžija, A. Popovič

Jožef Stefan Institute, Jamova 39, SI-1000 Ljubljana, Slovenia

Received 23 July 2008; received in revised form 25 September 2008; accepted 2 October 2008
Available online 8 November 2008

Abstract

The high-temperature behaviour of $K_{0.5}Bi_{0.5}TiO_3$, prepared using a conventional solid-state reaction method, was investigated using X-ray powder diffraction, scanning electron microscopy, wavelength-dispersive X-ray spectroscopy and Knudsen effusion combined with mass spectrometry. The results revealed the formation of an off-stoichiometric matrix phase with an excess of bismuth and a deficit of potassium compared to the stoichiometric $K_{0.5}Bi_{0.5}TiO_3$ during the solid-state reaction. During the thermal treatment potassium and bismuth vapours were detected over the solid sample and related to the thermal decomposition of the matrix phase. The losses of the potassium and bismuth components shifted the nominal composition to a three-phase region, and as a result, $K_2Ti_6O_{13}$ and a new Bi-rich ternary phase were formed in the system, the latter being formed after prolonged sintering. Differential thermal analyses and heating-microscope analyses showed a narrow sintering-temperature range limited by the melting of the sample above 1040 °C.

Keywords: $Bi_{0.5}K_{0.5}TiO_3$; Perovskites; Firing; Sintering; Inclusions

1. Introduction

Due to increasing restrictions on the use of lead-based electronic materials, research on piezoelectric ceramic materials has tended to focus more on lead-free materials. $Na_{0.5}Bi_{0.5}TiO_3$ and $K_{0.5}Bi_{0.5}TiO_3$ are two of the most interesting lead-free ferroelectrics, with relatively high temperatures of the permittivity maximum, i.e., 320 and 380 °C, respectively.[1,2] While the published work on $Na_{0.5}Bi_{0.5}TiO_3$ and its solid-solutions with $K_{0.5}Bi_{0.5}TiO_3$ is comprehensive,[3–6] only a few studies were conducted on the pure $K_{0.5}Bi_{0.5}TiO_3$ ceramic.[7–9] Recently, research work on $K_{0.5}Bi_{0.5}TiO_3$-based ceramics moved from solid-state-prepared powders to powders prepared by different chemical processes, such as sol–gel,[10,11] hydrothermal,[10,12] molten salt[13] or the polymerized complex[14] method. The literature suggests that the reason for the change in the synthesis route is to prepare finer, more homogeneous powders due to the difficulty in sintering dense, single-phase $K_{0.5}Bi_{0.5}TiO_3$ ceramics using a conventional process.

$K_{0.5}Bi_{0.5}TiO_3$ ceramics are usually prepared by the solid-state reaction method, consisting of a calcination stage below 1000 °C, where K_2CO_3, Bi_2O_3 and TiO_2 react with each other to form $K_{0.5}Bi_{0.5}TiO_3$,[7] and a sintering stage above 1000 °C.[6,8,9] Although the literature reports suggest a narrow sintering-temperature range, the reported sintering temperature of the solid-state-prepared powders varies from 1030[9] to 1120 °C.[6] Such a high sintering temperature is incompatible with the report of the sample melting at 1070 °C.[9] Secondary-phase formation during the synthesis of $K_{0.5}Bi_{0.5}TiO_3$ was observed; however, the identification of the secondary phase(s) formed in the system is inconsistent, as some papers report a $K_2Ti_6O_{13}$[9,15] secondary phase, while others identified $K_4Ti_3O_8$.[6,10–12] Because of the potassium and bismuth components present in the system, the possibility of volatilization was suggested. Despite this, volatilization in this system has not been investigated. Some authors predict the volatilization of potassium oxide,[8,14] while others predict the volatilization of bismuth oxide.[6,11,12] Furthermore, volatilization is assumed to be the main reason for the poor sinterability of $K_{0.5}Bi_{0.5}TiO_3$ ceramics.[8,12–14] In order to improve the sinterability of $K_{0.5}Bi_{0.5}TiO_3$ powders, different chemical processes[10–14] have been studied; however, the problems with secondary-phase formation and the narrow sintering-temperature range remain.

Since the melting temperature of $K_{0.5}Bi_{0.5}TiO_3$ ceramics was not yet determined, the reports of the volatile component are inconsistent and the secondary phases were identified only on

* Corresponding author. Tel.: +386 1 477 3481; fax: +386 1 477 3875.
E-mail address: jakob.konig@ijs.si (J. König).

0955-2219/$ – see front matter © 2008 Elsevier Ltd. All rights reserved.
doi:10.1016/j.jeurceramsoc.2008.10.002

the basis of weak reflections from XRD patterns, we performed a detailed investigation of the microstructure and the chemical composition of $K_{0.5}Bi_{0.5}TiO_3$ ceramics that should, together with XRD analyses, unambiguously confirm the identity of the secondary phase(s) and give us an insight into the processes that occur during the synthesis and sintering of $K_{0.5}Bi_{0.5}TiO_3$ powders. Additionally, the volatizing components and the melting temperature of $K_{0.5}Bi_{0.5}TiO_3$ prepared by the solid-state method were examined.

2. Experimental

$K_{0.5}Bi_{0.5}TiO_3$ powder was prepared using a solid-state reaction method. Stoichiometric amounts of reagent-grade K_2CO_3 (99.997% Alfa Aesar), Bi_2O_3 (99.975% Alfa Aesar) and TiO_2 (99.99% Alfa Aesar) were weighed and homogenized in a planetary mill, using 3-mm yttria-stabilized zirconia balls, at 200 rpm for 1 h under ethanol. Prior to weighing, the K_2CO_3 powder was dried at 200 °C for 4 h to remove any water content and cooled to room temperature in a silica-gel-filled desiccator. The homogenized powders were dried, uniaxially pressed into pellets under a pressure of 100 MPa and calcined in air at 750 and 850 °C for 10 h with intermediate cooling and grinding. The calcined samples were milled in the planetary mill at 200 rpm for 1 h under ethanol. The milled powders were then uniaxially pre-pressed (at 100 MPa) and cold isostatically pressed (at 750 MPa) into pellets and sintered at 1030 °C for various times. The sintering was performed in a tube furnace in an atmosphere of air with heating and cooling rates of 10 °C min^{-1}. Preliminary results showed that the sample reacts with alumina; therefore, all firings were performed on a gold foil. The density of the sintered samples was measured using Archimedes' method.

X-ray powder diffraction (XRD) was used to determine the phase structure of the samples after each firing. Room-temperature XRD patterns were recorded in the 2θ range 10–70° using a powder diffractometer with Cu Kα radiation in configuration with Johannson's monochromator to remove the Cu $K\alpha_2$ radiation (PANalytical X'Pert PRO). The typical step and step time used were 0.016° and 16 s, respectively. The microstructures of polished and fractured sintered samples were observed in a scanning electron microscope (SEM: JEOL JXA 840A and JSM 5800). Backscattered electron (BSE) imaging in the compositional contrast mode was applied to expose the presence of secondary phases in the $K_{0.5}Bi_{0.5}TiO_3$ matrix. The chemical composition of the samples was determined with electron-probe microanalysis using energy-dispersive (EDS) and wavelength-dispersive (WDS) X-ray spectroscopy. The EDS standardless quantitative analyses were performed at a 20-keV beam energy using a SEMQUANT program with a virtual standards package data library (EDS Oxford Instruments Link ISIS 300) and a ZAF matrix correction.

The accurate elemental composition of the $K_{0.5}Bi_{0.5}TiO_3$ matrix phase was determined with optimized, WDS quantitative microanalyses. The WDS measurements were carried out in a JXA 840A microanalyzer at 14 keV, with a 40-nA beam current and a 40° take-off angle. The intensities of the K-Kα, Bi-Mα and Ti-Kα spectral lines were measured using the PET crystal and the Xe-filled gas proportional counter. The standard reference materials were single crystals of $SrTiO_3$ and $KNbO_3$ and a polycrystalline Bi_2O_3 ceramic. The elemental k-ratios were quantified with conventional ZAF and Φ(ρz)-XPHI[16] matrix corrections. The oxygen content was calculated according to the nominal cation valency. High analytical precision was ensured with counting times set to achieve a counting error of less than 0.4% relative. The detection limits,[17] expressed in wt%, were low – 0.006 for K, 0.054 for Bi and 0.011 for Ti – which confirmed the high sensitivity attained with the WDS method and consequently allowed us to determine the elemental composition of the $K_{0.5}Bi_{0.5}TiO_3$ matrix with high accuracy.

The volatile species were determined using Knudsen effusion combined with mass spectrometry (KEMS).[18] In a typical experiment a sample (approximately 100 mg) was loaded in a platinum Knudsen cell and placed into the evaporator of a Nier-type mass spectrometer. After evacuation to 10^{-6} Pa the sample was first degassed at 120 °C. Next, the temperature was stepwise increased (10 °C min^{-1} heating rate, 5 min dwell time, before collecting data at the measured temperature) and the abundance of all the ion species that appeared in the mass spectrum was recorded. Finally, the equilibrium pressures of the neutral precursors were calculated using the following equation

$$p_i = k\left(\sum_j I^+_{i,j} T\right) \quad (1)$$

The symbols represent: $I^+_{i,j}$ – the jth ion abundance of a neutral precursor i/counts per second; p_i – the pressure of the neutral species/precursor i/Pa; T – the absolute temperature/K; k – the instrumental sensitivity constant that was determined in a separate experiment/(Pa K^{-1} Hz^{-1}).

The details of the method[18] and the experimental setup can be found elsewhere.[19]

The mass losses and the melting temperature of the sample were determined with thermogravimetric and differential thermal analyses (TGA and DTA) using a simultaneous thermal analysis instrument (STA 449 C/6/G Jupiter, Netsch). The experiments were performed in an atmosphere of air using platinum crucibles. The sintering of a compact sample, uniaxially compressed at 100 MPa, was observed by means of a heating microscope (EM201, Hesse Instruments). The heating rate in both experiments was 10 °C min^{-1}.

3. Results and discussion

The XRD analysis of the sample with the nominal composition $K_{0.5}Bi_{0.5}TiO_3$, calcined at 750 °C for 10 h, revealed that it contained a $K_{0.5}Bi_{0.5}TiO_3$ perovskite phase as well as some other crystalline phases (Fig. 1a). Though the reflections of the secondary phases are weak, the majority of the reflections were attributed to a $K_2Ti_4O_9$ phase. After a subsequent calcination at 850 °C for 10 h the XRD pattern shows the same characteristics (Fig. 1b); however, after sintering at 1030 °C for 5 h the positions of the weak reflections changed and were attributed to a $K_2Ti_6O_{13}$ secondary phase (Fig. 1c). The change in the sec-

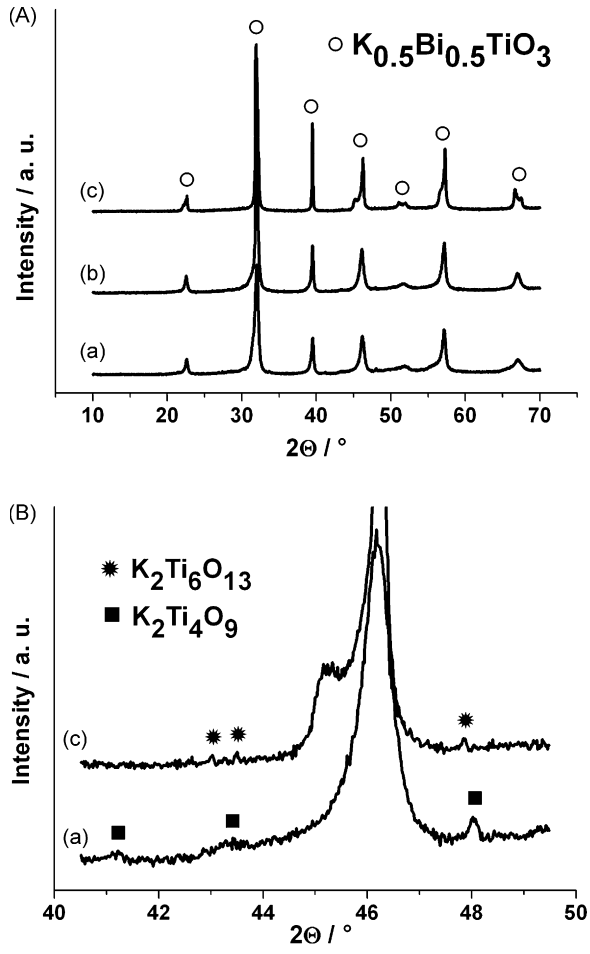

Fig. 1. (A) XRD patterns of the $K_{0.5}Bi_{0.5}TiO_3$ sample (a) after a 10 h calcination at 750 °C, (b) after a subsequent 10 h calcination at 850 °C and (c) after 5 h sintering at 1030 °C. (B) A detail of the XRD patterns (a) after the first calcination and (c) after sintering; the weak reflections of the $K_2Ti_4O_9$ and $K_2Ti_6O_{13}$ secondary phases are designated.

ondary phase will be discussed later in relation to the stability of potassium titanates. The SEM–BSE micrographs of the sintered sample clearly revealed the presence of a dark secondary phase in the form of whiskers (Fig. 2A). The composition of the dark phase, determined using EDS, corresponds to the $K_2Ti_6O_{13}$ phase, which is in accordance with the weak reflections observed in the XRD pattern (Fig. 1Bc).

With a prolonged 80-h sintering the concentration of the dark phase in the interior of the sample slightly increased; however, on the surface of the pellet the dark phase prevailed (Fig. 2B).

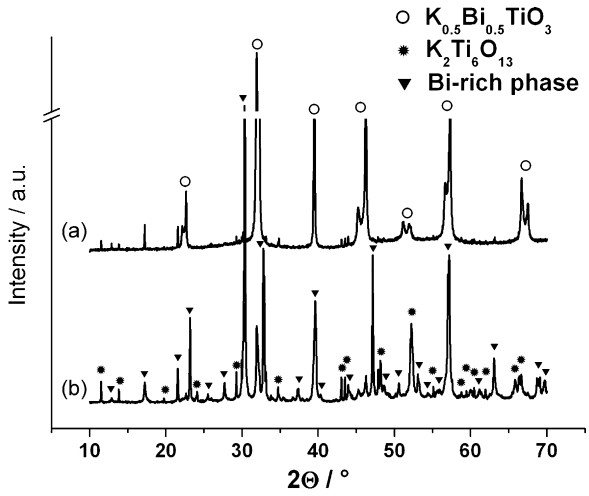

Fig. 3. XRD patterns of (a) $K_{0.5}Bi_{0.5}TiO_3$ powder fired at 1030 °C for 20 h and (b) K sample sintered at 1030 °C for 5 h. The reflections of $K_{0.5}Bi_{0.5}TiO_3$ are marked only on the (a) pattern; the reflections of $K_2Ti_6O_{13}$ and Bi-rich phase are marked only on the (b) pattern.

Furthermore, a bright secondary phase in the form of large, elongated grains (>100 μm in length) was formed, predominantly near to the surface of the sample. The EDS analysis of the bright phase suggested the composition $K_{0.1}Bi_{0.89}Ti_{0.81}O_3$. The bright phase will be hereafter referred to as the Bi-rich phase, since it contains more bismuth compared to the other phases. The SEM image of the fracture surface shows that even after prolonged sintering the matrix grains remained small, with an average size of approximately 1 μm (Fig. 2C).

These observations indicate that the formation of the secondary phases is accelerated on the surface of the pellet. Therefore, we performed an experiment on a powdered sample with an increased surface area, which enabled us to more accurately identify the secondary phases present. The finely ground, uncompressed, calcined $K_{0.5}Bi_{0.5}TiO_3$ powder was fired in air at 1030 °C for 20 h, and analyzed using XRD. Fig. 3a shows the pattern of the as-prepared sample. The main reflections belong to the $K_{0.5}Bi_{0.5}TiO_3$ perovskite phase, the second phase identified from the spectra is $K_2Ti_6O_{13}$, while the other reflections could not be identified on the basis of any file from the JCPDS database. The unidentified reflections are most probably connected with the Bi-rich phase, observed after prolonged sintering.

In order to get a clearer insight into the processes that occur during the synthesis of the $K_{0.5}Bi_{0.5}TiO_3$ ceramics, the phase relations around $K_{0.5}Bi_{0.5}TiO_3$ were investigated. Compositions

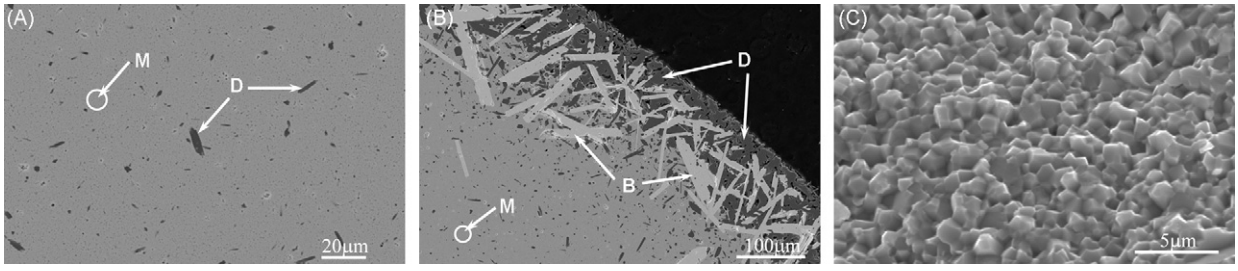

Fig. 2. SEM–BSE micrographs of the $K_{0.5}Bi_{0.5}TiO_3$ sample sintered at 1030 °C for (A) 5 h and (B) 80 h; M – matrix phase, D – $K_2Ti_6O_{13}$ (dark grains), B – Bi-rich secondary phase (bright grains) are designated. (C) A fracture surface of the $K_{0.5}Bi_{0.5}TiO_3$ sample sintered for 80 h.

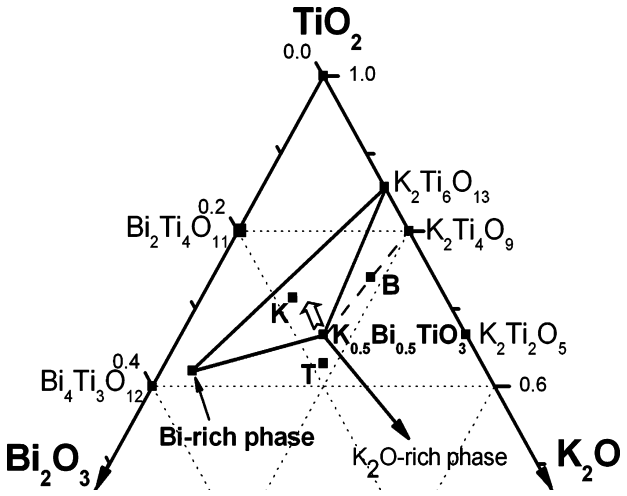

Fig. 4. Phase relations in the K_2O–Bi_2O_3–TiO_2 system at 1030 °C (solid lines) derived from the described experiments. The dashed line corresponds to 900 °C. The position of the Bi-rich phase is as determined by EDS. The open arrow marks the direction of a nominal composition change as a function of the sintering time.

with less potassium oxide ($K_{0.3}Bi_{0.5}TiO_{2.9}$ – K), bismuth oxide ($K_{0.5}Bi_{0.2}TiO_{2.55}$ – B) and titanium oxide ($K_{0.5}Bi_{0.5}Ti_{0.85}O_{2.7}$ – T) relative to $K_{0.5}Bi_{0.5}TiO_3$ were prepared and are shown in the phase diagram (Fig. 4). The pattern of sample K (with less potassium) shows weak reflections identified as $K_{0.5}Bi_{0.5}TiO_3$ and $K_2Ti_6O_{13}$; however, the main reflections could not be identified (Fig. 3b). These reflections are consistent with the unidentified reflections from the uncompressed $K_{0.5}Bi_{0.5}TiO_3$ powder fired at the sintering temperature, which are most probably connected to the Bi-rich phase. This was confirmed by the EDS analysis, which showed the same composition for the bright Bi-rich phase in sample K as in the $K_{0.5}Bi_{0.5}TiO_3$ pellet, and thus the unidentified peaks in Fig. 3a and b were denoted as the Bi-rich phase. The mismatch between the intensities of the peaks of the Bi-rich phase are most probably due to the different morphology of this phase observed with the SEM (isotropic in sample K and anisotropic in $K_{0.5}Bi_{0.5}TiO_3$). The XRD pattern of sample B (with less bismuth) fired at 900 °C for 5 h shows the presence of two phases, identified as $K_{0.5}Bi_{0.5}TiO_3$ and $K_2Ti_4O_9$; however, after firing at 1030 °C the intensity of the $K_2Ti_4O_9$ peaks decreased and the $K_2Ti_6O_{13}$ reflections appeared in the XRD pattern, which indicates the decomposition of the $K_2Ti_4O_9$ phase. The instability of $K_2Ti_4O_9$ was observed in a study of the synthesis of potassium titanate whiskers, where the decomposition of $K_2Ti_4O_9$ into $K_2Ti_6O_{13}$ whiskers and a K_2O-rich liquid phase is reported.[20] The authors report that the temperature of the $K_2Ti_4O_9$ decomposition in the TiO_2–K_2O system is around 1120 °C. Nevertheless, according to our experiments, the temperature of the decomposition of the $K_2Ti_4O_9$ phase in the investigated part of the K_2O–Bi_2O_3–TiO_2 system is below 1000 °C, while the $K_2Ti_6O_{13}$ phase appears in the form of whiskers, as reported in the literature. The XRD pattern of sample T contained the reflections of $K_{0.5}Bi_{0.5}TiO_3$; the other reflections in the XRD pattern of sample T could not be identified using the JCPDS database.

The above results confirmed that the $K_2Ti_6O_{13}$ secondary phase is present in $K_{0.5}Bi_{0.5}TiO_3$ ceramics. Also, no evidence was found for $K_4Ti_3O_8$, in contrast to some literature reports.[3,4,6,2] Furthermore, another ternary phase in $K_{0.5}Bi_{0.5}TiO_3$ ceramics, which has not been previously observed, is the Bi-rich phase that forms after prolonged sintering. Since the ternary phase-equilibrium diagram for the K_2O–Bi_2O_3–TiO_2 system has not been reported yet, we constructed phase relations around $K_{0.5}Bi_{0.5}TiO_3$ at 1030 °C on the basis of the described experiments (Fig. 4).

The firing of $K_{0.5}Bi_{0.5}TiO_3$ shifts the nominal composition to the three-phase region (marked by an open arrow in Fig. 4), which indicates the loss of potassium and bismuth oxides from the sample. In order to quantify the mass loss, a TGA analysis of the $K_{0.5}Bi_{0.5}TiO_3$ powder was performed. The analysis showed that as much as 6 wt% of the sample volatized over the 20-h period at 1030 °C. The volatilization during the sintering of the $K_{0.5}Bi_{0.5}TiO_3$ ceramics has been predicted in the literature; however, it is inconsistent, assuming that only the potassium component[8,14] or only the bismuth[6,11,12] component volatizes from the sample. Furthermore, there is no exact experiment documented that would confirm any volatilization. For this reason we used the Knudsen effusion mass spectrometry (KEMS) method to determine the volatile components at elevated temperatures. This method is a combination of the standard Knudsen effusion method and mass spectrometry.[18] The combined method makes it possible to identify gaseous species and determine their vapour pressure, being in thermodynamic equilibrium with the solid sample.

Two sets of KEMS experiments were performed, one on a previously calcined sample (750 and 850 °C for 10 h) and one on a starting carbonate/oxides mixture. In both cases the only metal-containing ionic species found in the mass spectrum were Bi^+, Bi^{++}, K^+ and BiO^+. The additional mass spectrometric measurements proved that those ions come from gaseous Bi, K and BiO, respectively. The concentration of the latter molecule is extremely low; therefore, we consider it to be of minor importance. For pure metal oxides in general, the formation of bismuth and potassium vapours within the Knudsen cell at the measured temperatures can be represented by the following equilibrium reactions:

$$K_2O(s) \leftrightarrow 2K(g) + \tfrac{1}{2}O_2 \quad (2)$$

$$Bi_2O_3(s) \leftrightarrow 2Bi(g) + \tfrac{3}{2}O_2 \quad (3)$$

The result of the KEMS measurements of the previously calcined sample can be seen in Fig. 5A. It is clear that the vapour pressure of bismuth is considerably higher than the pressure of potassium, being almost negligible compared to bismuth. Furthermore, the pressure of all the species monotonically increases with temperature when the dependence is plotted on a logarithmic scale. According to the phase diagram in Fig. 4, the complete loss of bismuth oxide would result in the formation of the pure $K_2Ti_4O_9$ phase. To verify this, the calcined sample was annealed in the mass spectrometer at 940 °C until the signal of bismuth disappeared from the mass spectra. The mass loss during annealing was found to be noticeably higher than the

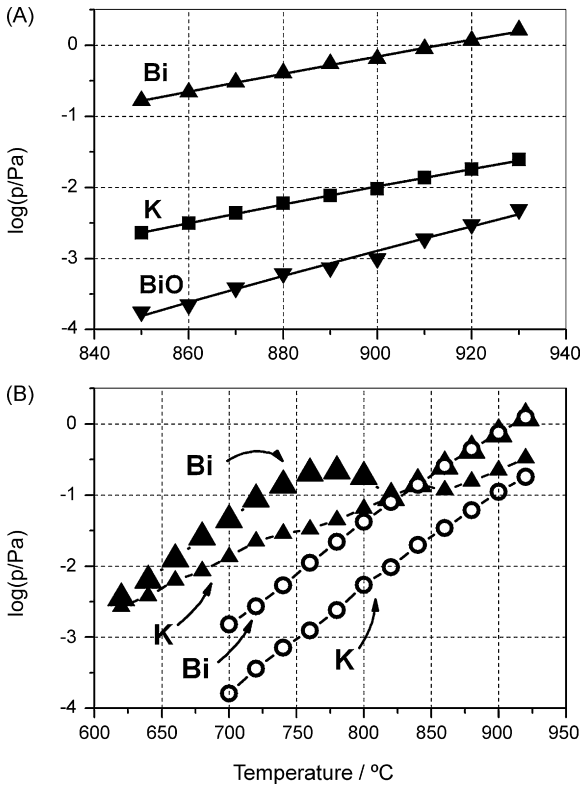

Fig. 5. (A) The measured vapour pressure of bismuth, potassium and bismuth oxide over calcined $K_{0.5}Bi_{0.5}TiO_3$. (B) The measured vapour pressure of bismuth and potassium over the Bi_2O_3, K_2CO_3, TiO_2 mixture (triangles: first run, open circles: second run).

content of bismuth oxide and, in addition, the remainder of the sample showed the presence of two potassium titanate phases, $K_2Ti_4O_9$ and $K_2Ti_6O_{13}$. Thus, the results also indicate a sizable volatilization of potassium oxide. Since the KEMS showed that the pressure of the potassium is considerably smaller than that of the bismuth during the annealing in the Knudsen cell, the majority of the potassium losses probably occurred during the calcinations. To investigate this, a second set of KEMS experiments was performed on a carbonate/oxides mixture. The result can be seen in Fig. 5B, where two successive runs are plotted on the graph. The first run is depicted with triangles. It is evident that at the early stage of the experiment (620 °C) the pressures of bismuth and potassium are similar. The increase of the potassium pressure with temperature is somewhat less steep, but it is still comparable to the bismuth, unlike in the case of the calcined sample. At higher temperatures (750–850 °C) a distinct drop in the bismuth pressure and a more gradual drop in the potassium pressure are observed, which might be related to the solid-state reaction. Finally, at 900 °C the system seems to reach thermodynamic equilibrium, which was checked with a subsequent run, designated by open circles in Fig. 5B (in between, the system was cooled to room temperature). In the second run the temperature–pressure dependence is monotonic for potassium and bismuth, which indicates the thermodynamic equilibrium of the system. It appears that the reaction is finished at this stage, and that essentially pure $K_{0.5}Bi_{0.5}TiO_3$ is in equilibrium with the vapours (the loss of components during the first run of this experiment is negligible). The pressure of the potassium over the carbonate/oxides mixture (second run) is about six times higher than over the calcined sample, where being considerably smaller than the pressure of the bismuth, which, in contrast, is almost identical in both cases. The drop in the pressure of potassium during the calcination can be related to the potassium losses detected in the first set of KEMS experiments on a previously calcined sample.

The described KEMS measurements were performed in vacuum. In order to apply the results to atmospheric conditions we have to consider the influence of oxygen on reactions (2) and (3). For the metal oxide decomposition (4)

$$\mathrm{Me}_a\mathrm{O}_b(\mathrm{s}) \leftrightarrow a\mathrm{Me}(\mathrm{g}) + \tfrac{b}{2}\mathrm{O}_2 \quad (4)$$

the dissociation constant can be calculated according to the following equation

$$K_{\mathrm{diss}} = (p_{\mathrm{Me}})^a (p_{\mathrm{O}_2})^{b/2} \quad (5)$$

where K_{diss} is the dissociation constant of reaction (4) and p_{O_2} and p_{Me} are the equilibrium pressures over solid $\mathrm{Me}_a\mathrm{O}_b$. Eq. (5) shows that the influence of the oxygen pressure in the surrounding atmosphere greatly influences the decomposition of metal oxides and the volatilization. If we take into consideration the a and b coefficients from reaction (4) for the potassium and bismuth volatilization described by reactions (2) and (3), we see that the presence of oxygen has a bigger influence on decreasing the volatilization of bismuth in comparison to potassium. Thus, the volatilization of potassium over the calcined sample (which is considerably smaller compared to the volatilization of bismuth in a vacuum) becomes important and comparable to the volatilization of bismuth in an atmosphere of air. It should be mentioned that the vapour pressure of both the potassium and bismuth components increases with temperature; therefore, most of the losses occur during the sintering of the samples, while the losses during calcinations are smaller.

The thermal instability of the $K_{0.5}Bi_{0.5}TiO_3$ matrix causes its slow decomposition and the volatilization of potassium and bismuth components; therefore, we decided to investigate the stoichiometry of the matrix phase. The EDS analyses of the samples sintered at 1030 °C for different times (5, 20 and 80 h) showed that in all the samples the $K_{0.5}Bi_{0.5}TiO_3$ matrix contained less potassium and more bismuth compared to the stoichiometric $K_{0.5}Bi_{0.5}TiO_3$. Because of the relatively low analytical sensitivity of the EDS method this deviation from the stoichiometric $K_{0.5}Bi_{0.5}TiO_3$ composition was additionally checked and determined with WDS. An accurate, quantitative WDS analysis of the $K_{0.5}Bi_{0.5}TiO_3$ matrix phase was performed on a sample sintered at 1030 °C for 20 h. The average composition of the matrix was determined from six point-beam analyses performed on randomly selected matrix grains. The composition of the $K_{0.5}Bi_{0.5}TiO_3$ matrix was calculated using the quantitative WDS data obtained from two quantitative matrix-correction methods, XPHI and ZAF, and can be described by $K_{0.478\pm0.002}Bi_{0.508\pm0.002}Ti_{1.000\pm0.002}O_3$ and $K_{0.477\pm0.002}Bi_{0.509\pm0.002}Ti_{0.999\pm0.002}O_3$, respectively. Both formulas are consistent and equivalent within the range of statistical

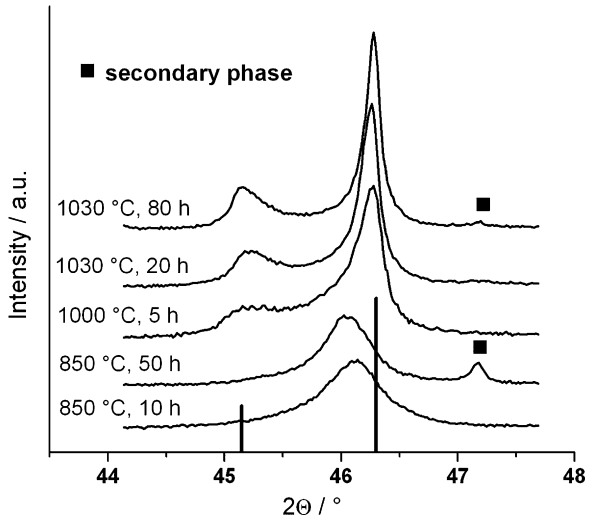

Fig. 6. XRD results of $K_{0.5}Bi_{0.5}TiO_3$ samples fired at different temperatures for different times. The vertical lines represent the diffraction lines of $K_{0.5}Bi_{0.5}TiO_3$ according to PDF card number 36-0339.

uncertainty. The relative standard deviation of the formula coefficients, calculated from elemental concentrations, is less than 0.3% (between the points), and is similar to the relative counting error or precision of the WDS analysis, which also confirms that the $K_{0.5}Bi_{0.5}TiO_3$ matrix is compositionally homogeneous. The presented results clearly show that the synthesized $K_{0.5}Bi_{0.5}TiO_3$ compound is not stoichiometric $K_{0.5}Bi_{0.5}TiO_3$; it is potassium-deficient and contains an excess of bismuth.

The non-stoichiometry in $K_{0.5}Bi_{0.5}TiO_3$ has not been reported before; however, A-site deficiency was documented in a related $Na_{0.5}Bi_{0.5}TiO_3$ compound, where sodium deficiency was connected with the pseudo-cubic symmetry of $Na_{0.5}Bi_{0.5}TiO_3$.[21] The authors found a stable sodium-deficient compound that forms a solid-solution with $Na_{0.5}Bi_{0.5}TiO_3$ and the formation of stoichiometric $Na_{0.5}Bi_{0.5}TiO_3$ starts with the formation of the sodium-deficient end-member, which then reacts toward the nominal composition when a sufficiently high temperature and/or a long firing time is used. A similar crystal-symmetry variation with the firing temperature was also observed for $K_{0.5}Bi_{0.5}TiO_3$. The symmetry of the $K_{0.5}Bi_{0.5}TiO_3$ is pseudo-cubic after the calcinations, and this changes to tetragonal during the sintering at higher temperatures (Fig. 6). Due to the similarity with $Na_{0.5}Bi_{0.5}TiO_3$, the existence of a solid-solution around $K_{0.5}Bi_{0.5}TiO_3$ was investigated. The symmetry of $K_{0.5}Bi_{0.5}TiO_3$ and the compositions K, B and T, heat treated at different temperatures and for different firing times, was carefully investigated by XRD. The analysis showed a pseudo-cubic symmetry after the calcinations and a tetragonal symmetry after the sintering for all samples, and furthermore, the positions of the reflections were identical. Therefore, we concluded that the stoichiometry of the synthesized compound is always the same and there is no evidence of a solid-solution existing around that compound.

The results of the WDS and the crystal-structure analyses showed that an off-stoichiometric matrix phase, compared to

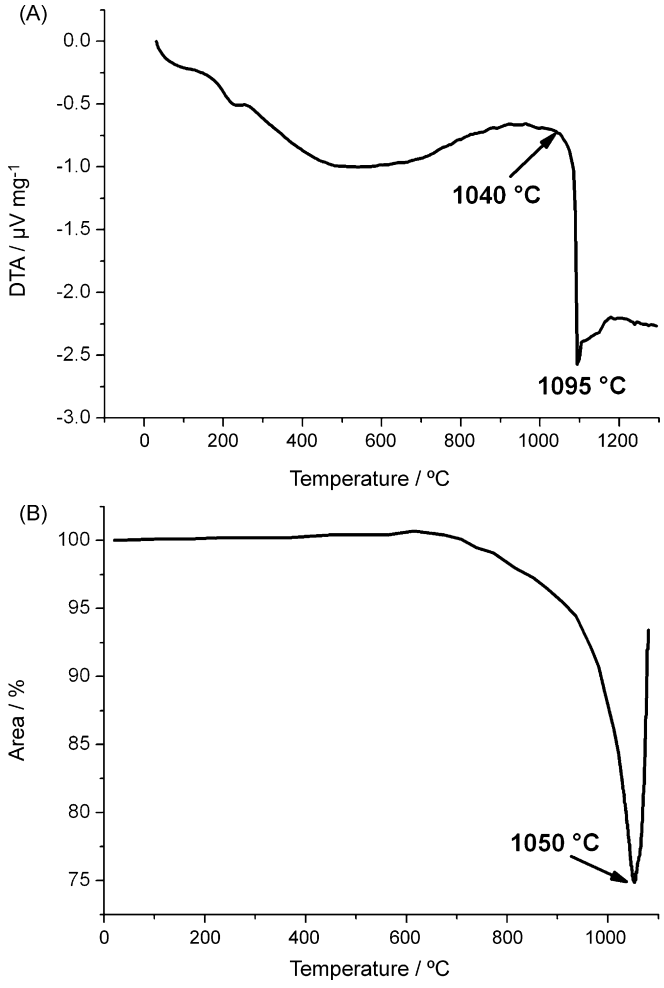

Fig. 7. The results of (A) the DTA and (B) the heating-microscope analysis.

$K_{0.5}Bi_{0.5}TiO_3$, forms in the system and that there is no solid solution around it. Rather, it appears that only a discrete composition forms in the system, which has a stoichiometry slightly shifted from the ideal one, i.e., from $K_{0.5}Bi_{0.5}TiO_3$. Thus, during the sintering the matrix phase slowly decomposes and forms the $K_2Ti_6O_{13}$ and Bi-rich secondary phases (as observed by XRD and SEM analyses), as well as Bi and K vapours above the solid sample (as determined by TGA and KEMS).

The melting temperature of the $K_{0.5}Bi_{0.5}TiO_3$ powders and the sintering behaviour of the $K_{0.5}Bi_{0.5}TiO_3$ compact were investigated by means of DTA and a heating microscope. The DTA curve (Fig. 7A) shows that the endothermic signal ascribed to the melting of the sample starts at 1040 °C and peaks at 1095 °C. The heating-microscope analysis (Fig. 7B) shows the maximum shrinkage of the compact at 1050 °C, while at higher temperatures the sample starts to melt and it completely deforms at 1070 °C (hemisphere point). The results of the DTA and the heating-microscope analysis are in good agreement and show that the sintering-temperature range is narrow, limited by the melting of the sample above 1040 °C and the low density of the ceramics below 1030 °C. On the basis of these results, we determined the sintering temperature in our experiments to be 1030 °C. At this temperature, the optimal ratio between the

density of the ceramic compact and the secondary-phase concentration was observed. The densities of $K_{0.5}Bi_{0.5}TiO_3$ samples sintered at 1030 °C for 5 and 20 h were 92 and 96%, respectively, of the theoretical density of $K_{0.5}Bi_{0.5}TiO_3$. The as-prepared $K_{0.5}Bi_{0.5}TiO_3$ ceramics are of sufficient quality for a proper electrical characterization.

4. Conclusion

The results showed the volatilization of the potassium and bismuth components during the preparation of $K_{0.5}Bi_{0.5}TiO_3$ ceramics. The thermal decomposition of the sample induces a shift of the nominal composition to a composition within the corresponding three-phase region and, consequently, secondary phases are formed, i.e., $K_2Ti_6O_{13}$ and a new Bi-rich ternary phase. The WDS analysis revealed that the matrix phase is non-stoichiometric, with a deficit of potassium and an excess of bismuth compared to the nominal $K_{0.5}Bi_{0.5}TiO_3$. The sintering temperature range is narrow, limited by the melting of the sample above 1040 °C, and, therefore, for a successful sinter the sintering temperature has to be carefully selected to achieve an appropriate density of the ceramics, as well as the lowest secondary-phase concentration.

Acknowledgement

The research was financially supported by the Ministry of Higher Education, Science and Technology of the Republic of Slovenia, under Grant No. 3311-04-831066.

References

1. Tu, T. S., Siny, I. G. and Schmidt, V. H., Sequence of dielectric anomalies and high-temperature relaxation behavior in $Na_{1/2}Bi_{1/2}TiO_3$. *Phys. Rev. B*, 1994, **49**(17), 11550–11559.
2. Takenaka, T. and Nagata, H., Current status and prospects of lead-free piezoelectric ceramics. *J. Eur. Ceram. Soc.*, 2005, **25**, 2693–2700.
3. Elkechai, O., Manier, M. and Mercurio, J. P., $Na_{0.5}Bi_{0.5}TiO_3$-$K_{0.5}Bi_{0.5}TiO_3$ (NBT–KBT) system: a structural and electrical study. *Phys. Stat. Sol. A*, 1996, **157**, 499–506.
4. Jones, G. O., Kreisel, J. and Thomas, P. A., A structural study of the $(Na_{1-x}K_x)_{0.5}Bi_{0.5}TiO_3$ perovskite series as a function of substitution (x) and temperature. *Powder Diffr.*, 2002, **17**(4), 301–319.
5. Said, S. and Mercurio, J. P., Relaxor behavior of low lead and lead free ferroelectric ceramics of $Na_{0.5}Bi_{0.5}TiO_3$–$PbTiO_3$ and $Na_{0.5}Bi_{0.5}TiO_3$–$K_{0.5}Bi_{0.5}TiO_3$ systems. *J. Eur. Ceram. Soc.*, 2001, **21**, 1333–1336.
6. Zhao, S., Li, G., Ding, A., Wang, T. and Yin, Q., Ferroelectric and piezoelectric properties of $(Na, K)_{0.5}Bi_{0.5}TiO_3$ lead free ceramics. *J. Phys. Appl. Phys.*, 2006, **39**, 2277–2281.
7. Zaremba, T., Application of thermal analysis to study of the synthesis of $K_{0.5}Bi_{0.5}TiO_3$ ferroelectric. *J. Therm. Anal. Calorim.*, 2003, **74**, 653–658.
8. Wada, T., Toyoike, K., Imanaka, J. and Matsuo, Y., Dielectric and piezoelectric properties of $(A_{0.5}Bi_{0.5})TiO_3$–$ANbO_3$ (A = Na, K) systems. *Jpn. J. Appl. Phys.*, 2001, **40**(9B), 5703–5705.
9. Himura, Y., Aojagi, R., Nagata, H. and Takenaka, T., Ferroelectric and piezoelectric properties of $(Bi_{1/2}K_{1/2})TiO_3$ ceramics. *Jpn. J. Appl. Phys.*, 2005, **44**(7A), 5040–5044.
10. Hou, Y. D., Hou, L., Huang, S. Y., Zhu, M. K., Wang, H. and Yan, H., Comparative study of $K_{0.5}Bi_{0.5}TiO_3$ nanoparticles derived from sol–gel hydrothermal and sol–gel routes. *Solid State Commun.*, 2006, **137**, 658–661.
11. Li, Z. F., Wang, C. L., Zhong, W. L., Li, J. C. and Zhao, M. L., Dielectric relaxor properties of $K_{0.5}Bi_{0.5}TiO_3$ ferroelectrics prepared by sol–gel method. *J. Appl. Phys.*, 2003, **94**(4), 2548–2552.
12. Hou, L., Hou, Y. D., Song, X. M., Zhu, M. K., Wang, H. and Yan, H., Sol–gel-hydrothermal synthesis and sintering of $K_{0.5}Bi_{0.5}TiO_3$ nanowires. *Mater. Res. Bull.*, 2006, **41**, 1330–1336.
13. Yang, J., Hou, J., Wang, C., Zhu, M. and Yan, H., Relaxor behavior of $K_{0.5}Bi_{0.5}TiO_3$ ceramics derived from molten salt synthesizes single-crystalline nanowires. *Appl. Phys. Lett.*, 2007, **91**, 023118.
14. Wada, T., Fukui, A. and Matsuo, Y., Preparation of $(K_{0.5}Bi_{0.5})TiO_3$ ceramics by polymerized complex method and their properties. *Jpn. J. Appl. Phys.*, 2002, **41**(11B), 7025–7028.
15. Gao, F., Zhang, C. S., Zhao, M., Wang, W. M. and Tian, C. S., Microstructure and piezoelectric properties of $(Na_{0.85}K_{0.15})_{(0.5)}Bi_{0.5}TiO_3$ lead-free ceramics prepared by tape casting processing. *J. Inorg. Mater.*, 2006, **21**(5), 1134–1140.
16. Merlet, C., Quantitative electron probe microanalysis: new accurate $\Phi(\rho z)$ description. *Mikrochim. Acta*, 1992, **12**, 107–113.
17. Ziebold, T. O., Precision and sensitivity in electron microprobe analysis. *Anal. Chem.*, 1967, **39**, 858–861.
18. HTMS Drowart, J., Chatillon, C., Hastie, J. and Bonnel, D., High-temperature mass spectrometry: instrumental techniques, ionization cross-sections, pressure measurements, and thermodynamic data. *Pure Appl. Chem.*, 2005, **77**(4), 683–737.
19. Popovič, A., Mass spectrometric determination of the ionization cross-sections of BaO, Ba, BaF_2 and BaI_2 by electron impact. *Int. J. Mass Spectrom.*, 2003, **230**, 99–112.
20. Bao, N. Z., Feng, X., Lu, X. H. and Yang, Z. H., Study of the formation and growth of potassium titanate whiskers. *J. Mater. Sci.*, 2002, **37**, 3035–3043.
21. Spreitzer, M., Valant, M. and Suvorov, D., Sodium deficiency in $Na_{0.5}Bi_{0.5}TiO_3$. *J. Mater. Chem.*, 2007, **17**, 1–9.